Scientia Iranica B (2017) 24(5), 2387–2395

Sharif University of Technology
Scientia Iranica
Transactions B: Mechanical Engineering
www.scientiairanica.com

Theoretical and computational investigation of optimal wall shear stress in bifurcations: A generalization of Murray's law

M. Golozar[a], M. Sayed Razavi[a] and E. Shirani[b,*]

a. *Department of Mechanical Engineering, Isfahan University of Technology, Isfahan, P.O. Box 84156-83111, Iran.*
b. *Department of Engineering, Foolad Institute of Technology, Fooladshahr, Isfahan, P.O. Box 84916-63763, Iran.*

Received 12 September 2015; received in revised form 8 July 2016; accepted 30 July 2017

KEYWORDS
Wall shear stress;
Murray's law;
Turbulent flow;
Flow resistance;
Blood regulation.

Abstract. This paper investigates the optimal distribution of Wall Shear Stress (WSS) in a bifurcation and its effect on the morphology of blood vessels. The optimal WSS is obtained through minimization of energy loss due to friction and metabolic consumption. It is shown that the optimal WSS is a function of metabolic rate, fluid properties, diameter, and flow regime. For fully developed laminar and turbulent flows, different patterns of WSS are observed. The WSS is shown to be constant for the laminar flow, while it is a function of the tube diameter for the turbulent flow, in which the exponent of diameter varies with the tube relative roughness. Based on the optimal WSS and conservation of mass, the optimal relationship between diameters of mother and daughters' vessels is obtained for different flow regimes. Also, it is theoretically shown that the optimal distribution of WSS in a bifurcation minimizes flow resistance as well as energy loss. In addition, it is demonstrated that the specific relationship between the length and diameters of a blood vessel and optimal relationship between diameters lead to the optimal WSS distribution. Finally, the numerical simulation is used to investigate the effect of Reynolds number on the optimal WSS and flow resistance and to verify the theoretical formula predictions, obtained in this work.

1. Introduction

Optimality principles in arterial branching have often been studied to predict the relationships between diameters and bifurcation angles of arterial junctions since Murray's work in the 1920s [1,2]. Based on the principle of minimum energy and conservation of mass, Murray formulated a relationship between the diameter of the mother vessel and the diameters of the daughter vessels [1,3]. This relationship links the diameter of the mother vessel to that of the daughter vessels as $D_0^3 = D_1^3 + D_2^3$, where D_0, D_1, and D_2 are the diameters of the parent and two daughter vessels, respectively. Based on Murray's law, cost function is the sum of the rate at which work is done on the blood and the rate at which energy is used up by the blood vessel due to metabolism [3]. By minimizing the cost function with respect to the radius, he obtained $Q = kD^3$, where Q and D denote the volumetric flow rate and the diameter of a vessel segment, respectively, and k is a constant. A generalization of this relation can be proposed as $Q = kD^C$ where C is a constant and is determined based on fluid properties and energetic principles, i.e. exponent 2 ($Q = kD^2$) corresponds

*. *Corresponding author. Tel.: +98 3113915205; Fax: +98 3113912628*
E-mail address: eshirani@ictp.it (E. Shirani)

doi: 10.24200/sci.2017.4506

to conservation of the area, and thus constant flow velocity in and out of the bifurcation [4,5]. Exponents greater than 2 suggest a decrease in flow velocity, while exponents less than 2 imply an increase in flow velocity downstream of the bifurcation. Therefore, applying the Murray's law at the bifurcation leads to the decrease of mean velocity downstream of the bifurcation [5]. Furthermore, the shear stress on the vessel walls is uniform and independent of vessel diameter for laminar regimes, where $C = 3$ [6]. Uylings [7] argued that exponent C can vary in the range of 2.33 to 3.0 depending on whether the flow is turbulent (in large arteries) (2.33) or laminar (3.0) [8]. The optimization model suggested by Uylings was derived from minimal energy loss due to frictional resistance of laminar and turbulent flows and the volume of the duct system [7]. Numerous papers have been published in the past century on Murray's law and the validation of the exponent. Although some studies support the exponent predicted by Murray's law, the value of exponent has been debated for different anatomical districts and species.

However, it also has been reported by some investigators that the assumption of constant wall shear stress throughout the vasculature predicted by Murray's law may not be realistic, and exponent 3 in Murray's law must be replaced by different exponents [4,9]. In vivo measurements of the exponent for different arteries, it has been shown that the real exponent of Murray's law is about 2 for aortic bifurcation, 2.5 to 3 for coronary, 2.9 in carotid bifurcation, and about 3 in arterioles [5,9-11].

Furthermore, in the upper airways of the lung, turbulent flow exists during inspiration, which changes to laminar flow in the lower airways [7]. The blood flow in the aorta of, for instance, normal rabbits and humans is turbulent under some circumstances which changes to laminar flow in the arteries. Different types of flow are thus present in both lung and vascular tree structures [7].

The objective of this study is to determine the effect of the optimal pattern of WSS on the design of a bifurcation of a blood vessel for different flow regimes. A general formulation was obtained for the distribution of the optimal WSS in the microvascular bifurcation. Furthermore, an extension of Murray's law as a function of diameter and flow regime was developed. Also, the necessary and sufficient condition of blood vessels architecture for providing the optimal pattern of WSS was discussed. Based on the minimization of flow resistance, the optimal relationship between mother and daughter was interpreted as a flow architecture, providing minimal flow resistance. Moreover, to verify the theoretical formula predictions, the effect of Reynolds number on the optimal WSS and the flow resistance was numerically investigated.

2. Methods

2.1. Structure and geometry of vessel walls

Arteries and veins are mainly composed of three layers called intimal, media, and adventitia that surround the lumen of blood vessels. The intima, which is in intimate contact with blood, contains endothelium that lines the lumen of the vessel, enabling blood vessel to sense shear stress. Flow-induced changes in vessel caliber tend to restore baseline WSS and have been reported to be endothelium-dependent [12]. Endothelium lining the cardiovascular system is highly sensitive to hemodynamic shear stresses that act at the vessel luminal surface in the direction of blood flow. Physiological variations of shear stress regulate acute changes in the vascular diameter, while pathological shear stress results in maladaptive growth and the structural remodeling [13]. Regions of flow disturbances near arterial branches, bifurcations, and curvatures result in complex spatiotemporal shear stresses and their characteristics can predict atherosclerosis susceptibility. Changes in local artery geometry during atherogenesis further modify shear stress characteristics at the endothelium [13].

Furthermore, in order to study the effects of optimality and efficiency in cardiovascular system, it is necessary to consider the close vicinity of junction points as it is the most important part in the geometry of blood vessels. Similar to Zamir's work [14], the branching geometry at a junction is defined in terms of the tangents to the center lines of the vessels at the junction point [14]. Additionally, in the close vicinity of the junction point, the vessels are considered to be straight longitudinally with their walls parallel to the tangents of their respective center lines at the junction point [14]. This is clearly an approximation that leads to the tree-shaped flow structure model, which is a simplified model to study hemodynamic phenomena both experimentally and theoretically. The tree-shaped bifurcation can be symmetrical or asymmetrical. In this study, a bifurcation with two daughter branches is selected, where L_0 and D_0 refer to the length and diameter of the mother branch; L_1, D_1, and L_2, D_2 are also the length and diameter of the first and second daughter branches, respectively.

2.2. Optimum design of blood vessel bifurcation

2.2.1. Volumetric flow rate and viscous loss

Friction factor as a function of Reynolds number for different flow regimes can be written as follows:

$$C_f = \frac{\tau_w}{\frac{1}{2}\rho u^2} = \frac{g}{\mathrm{Re}^n}. \tag{1}$$

In the above equation, g and n are determined by flow regimes. For laminar and turbulent regimes, g and n

depend on Reynolds number and wall properties. Using Eq. (1) and the definition of Reynolds number ($\mathrm{Re} = \frac{\mathrm{VD}}{v}$), flow rate ($Q$) and power loss due to friction in the conduit (ϕ) can be calculated as follows:

$$Q = \lambda(\tau_w D^{4-n})^{\frac{1}{2-n}}, \tag{2}$$

$$\phi = \eta L \tau_w^{\frac{n-3}{n-2}} D^{\frac{2}{2-n}}, \tag{3}$$

where $\lambda = (2g\pi^{n-2}\upsilon^n\rho)^{\frac{1}{n-2}}$ and $\eta = 4 \times (2g\pi^{(n-2)}\upsilon^n\rho)^{\frac{1}{n-2}}$ are constants for blood. For details, see Appendices A and B.

2.2.2. Optimal WSS distribution

In biological systems, there are usually two terms of energy loss. The first loss, Φ, is the energy required to pump fluid through the conduit to overcome viscous losses. The second term can be related to the cost function at which energy is used up through blood vessels by metabolism [3]. Hence, the total energy loss in the system can be found by summing the viscous and metabolic components as given below:

$$E_{\mathrm{global}} = \phi + \Gamma\left(\frac{\pi D^2}{4}L\right), \tag{4}$$

where Φ is power loss, Γ is metabolic rate, and D and L are the diameter and length of conduit, respectively.

The global energy in Eq. (4) can be expressed as follows:

$$E_{\mathrm{global}} = \alpha D^{\frac{n-5}{n-2}} L^{\frac{1}{n-2}} (\Delta P)^{\frac{n-3}{n-2}} + \Gamma\left(\pi\frac{D^2}{4}L\right), \tag{5}$$

where $\alpha = 32^{\frac{1}{n-2}}(4^{-n}g\pi^{n-2}\upsilon^n\rho)^{\frac{1}{n-2}}$ is a constant.

At constant diameter of the vessel, constant pressure difference along the vessel, and constant metabolic rate, total energy, E_{global}, is a minimum when:

$$L = \Psi\frac{\Delta P}{D^{\frac{n+1}{n-3}}}, \tag{6}$$

where $\Psi = (\frac{4\alpha}{(2-n)\pi\Gamma})^{\frac{n-2}{n-3}}$ is a constant.

Finally, by using the definition of WSS, $\tau_w = \frac{\Delta \mathrm{P.D}}{4L}$, the optimal WSS can be expressed as follows:

$$\tau_w = \beta D^{\frac{2(n-1)}{n-3}}, \tag{7}$$

where $\beta = (-8^{\frac{n}{n-2}}\Gamma(n-2)(g\upsilon^n\rho)^{-\frac{1}{n-2}})^{\frac{n-2}{n-3}}$ is a constant.

From Eq. (7), we can see that for laminar flow, where $n = 1$, the wall shear stress through a conduit is only a function of fluid properties. With the transition from laminar to turbulent flow, the value of n becomes continuously smaller and the exponent of the conduit's diameter becomes larger; in addition, with $n = 0$ as the limit in the case of fully turbulent flow, the exponent of the conduit's diameter is 2/3.

Consequently, WSS for turbulent flow depends on the diameter of the conduit, and it increases with the increase of the diameter.

By using Eq. (7) for mother and daughter vessels, the relationship between mother and daughter's WSS is obtained as follows:

$$\frac{\tau_{\mathrm{wall,daughter}}}{\tau_{\mathrm{wall,mother}}} = \left(\frac{D_d}{D_m}\right)^{\frac{2(n-1)}{n-3}}. \tag{8}$$

It is obvious that for laminar flow, where $n = 1$, WSS of the mother conduit is the same as that of the daughter conduit, and for $0 \le n \le 1$, this ratio is dependent on the ratio of the diameters, resulting in a different WSS in mother and daughter vessels.

2.2.3. Optimal relationship of diameters between mother and daughter branches

By substituting WSS from Eq. (6) into Eq. (2) (see Appendix B), the volumetric flow rate of a conduit can be expressed as a function of conduit's diameter as follows:

$$Q = \kappa D^{\left(\frac{n-7}{n-3}\right)}, \tag{9}$$

where $\kappa = \lambda\beta^{-\frac{1}{n-2}}$ is a constant. The optimum relationship between the diameter of parent, D_0, and daughter branches, D_1 and D_2, can be derived from Eq. (9) using the principle of conservation of mass at the bifurcation point:

$$D_0^{\left(\frac{n-7}{n-3}\right)} = D_1^{\left(\frac{n-7}{n-3}\right)} + D_2^{\left(\frac{n-7}{n-3}\right)}. \tag{10}$$

This relationship is a general extension of Murray's law for flow in arterial bifurcations. Different relationships derived by substituting the respective values of n in Eq. (10) are summarized in Table 1. Also, the above equation can be verified by the result presented in the work of Uylings.

2.2.4. Geometric conditions for providing the optimal WSS distribution

Eq. (10) was derived under the assumption of the optimal WSS in the bifurcation. This argument would only be valid if we obtain Eq. (10) from the assumption of the optimal WSS. It is indispensable to understand that the reverse conclusion does not necessarily hold true. In other words, if the optimal relationship between mother and daughter vessels (Eq. (10)) exists in a bifurcation, we cannot conclude that WSS is optimal. Further assumption is required to infer such an implication.

Using Eqs. (1) and (7) and conservation of mass ($Q_0 = Q_1 + Q_2$) for a bifurcation (see Appendix E)

Table 1. Optimal geometrical relationship between daughter and mother vessels.

Flow regime	Relationship for diameters	Relationship between diameters and lengths
Laminar	$D_0^3 = D_1^3 + D_2^3$	$L_1/D_1 = L_2/D_2$
Turbulent (smooth) $\left(n = \frac{1}{4}\right)$	$D_0^{\frac{27}{11}} = D_1^{\frac{27}{11}} + D_2^{\frac{27}{11}}$	$L_1/D_1^{\frac{5}{11}} = L_2/D_2^{\frac{5}{11}}$
Turbulent (rough) $(n = 0)$	$D_0^{\frac{7}{3}} = D_1^{\frac{7}{3}} + D_2^{\frac{7}{3}}$	$L_1/D_1^{\frac{1}{3}} = L_2/D_2^{\frac{1}{3}}$

results in the optimal WSS in the bifurcation as follows:

$$\frac{L_0}{D_0^{\frac{n+1}{3-n}}} = \frac{L_1}{D_1^{\frac{n+1}{3-n}}} = \frac{L_2}{D_2^{\frac{n+1}{3-n}}}, \tag{11}$$

$$D_0^{\left(\frac{n-7}{n-3}\right)} = D_1^{\left(\frac{n-7}{n-3}\right)} + D_2^{\left(\frac{n-7}{n-3}\right)}. \tag{12}$$

It is obvious that for laminar flows, where $n = 1$, Eq. (10) is the same as Murray's law, and Eq. (11) becomes $L_0/D_0 = L_1/D_1 = L_2/D_2$. Consequently, in order to obtain the optimal WSS in a bifurcation, in addition to Eq. (10), the ratio of the length and diameter of the mother vessel must be equal to the ratio of the length and diameter of the daughter vessel. The results of the above equation for different values of n are summarized in Table 1.

2.2.5. The optimal architecture and minimal flow resistance

Constructal theory states that natural flow systems have evolved, such that they provide easier access to global flow [15,16]. In this regard, the architecture of an optimal vascular system should minimize flow resistance to provide easier access of blood flow. In other words, for vascular systems, the flow resistance must be minimized [5]. Minimization of flow resistance ($R_s = \Delta p/Q^{2-n}$) of a tree-shaped bifurcation (see Appendix D) results in:

$$\frac{L_1}{D_1^{\frac{n+1}{3-n}}} = \frac{L_2}{D_2^{\frac{n+1}{3-n}}}, \tag{13}$$

$$D_0^{\left(\frac{n-7}{n-3}\right)} = D_1^{\left(\frac{n-7}{n-3}\right)} + D_2^{\left(\frac{n-7}{n-3}\right)}. \tag{14}$$

Comparing Eqs. (11) and (12) and Eqs. (12) to (14) shows that minimizing energy loss provides minimal flow resistance in the bifurcation as well.

2.3. Numerical simulation

The effects of Reynolds number on WSS distribution and flow resistance are investigated for laminar flows. In addition, the effects of the ratio of mother and daughter diameters on flow resistance with respect to different Reynolds numbers are considered.

The geometry of the bifurcation is symmetrical with a mother and two identical daughter branches. Radius and length of the mother branch are 0.5 cm and 5 cm, respectively, similar to Aorta vessels [5,6]. Also, the ratio of the diameter and length of the daughter to mother branches are $D_d/D_m = 2^{-1/3} \cong 0.8$ and $L_d/L_m = 2^{-1/3}$, respectively. For comparison, different geometries were chosen under the assumption of equal occupied volumes. Under this assumption, different ratios of daughter to mother diameters (D_d/D_m) were chosen as 0.4, 0.5, 0.6, 0.7, 0.9, and 1.

The blood flow was assumed to be steady, laminar, and incompressible. An average velocity at the inlet and zero pressure ($P_{\text{out}} = 0$) at the outlet were assigned. The density and viscosity of blood are 1050 kg/m^3 and 0.00345 pa.s, respectively [17]. Also, the wall was assumed to be rigid. Furthermore, the average velocity at the inlet was selected as 50 cm/s, 5 cm/s, and 0.5 cm/s; the corresponding Reynolds numbers are 1400, 140, and 14. A 3-D finite-element numerical algorithm was used to obtain the distribution of the pressure and velocity fields of the blood flow in the bifurcation. The governing equations are expressed as follows:

$$\nabla \cdot \bar{u} = 0, \tag{15}$$

$$\rho \bar{u} \cdot \nabla \cdot \bar{u} = \nabla \cdot P + \mu \nabla^2 \bar{u}, \tag{16}$$

where P, ρ, and μ are the fluid pressure, density, and viscosity, respectively.

3. Results and discussion

The effects of Reynolds number and geometrical parameters on the optimal WSS and the flow resistance were investigated. Figure 1(a)-(c) show velocity distribution for an idealized geometry of Aorta bifurcations. As shown in this figure, with the increase of Reynolds number, the maximum velocity in the daughter vessel deviates and gets closer to the inner wall of the vessel. In addition, we notice from Figure 2 that streamlines deviate at the junction point, and as the Reynolds number increases, they get closer to the inner wall of the vessel. In fact, as the Reynolds number increases,

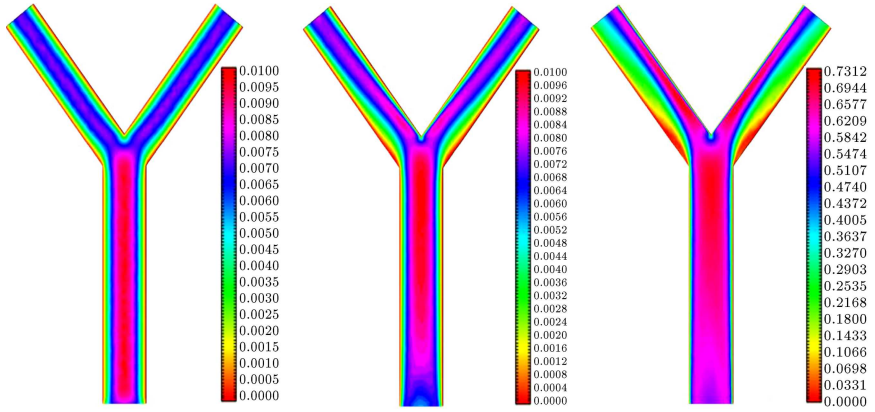

Figure 1. Velocity distribution and blood flow pattern in aorta geometry with the diameter ratio of 0.8 for: (a) Re = 14; (b) Re = 140 and (c) Re = 1400.

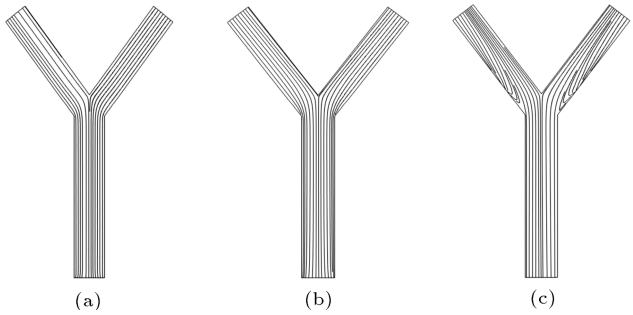

Figure 2. Streamlines of blood flow in aorta geometry with the diameter ratio of 0.8 for (a) Re = 14 (b) Re = 140, and (c) Re = 1400.

the effects of inertia become important in the close vicinity of the junction point. Consequently, as a result of inertia effects, the velocity profile deviates at the junction point. As can be seen in Figure 1(b), the velocity is higher near the interior wall of the junction and it is lower near the outer wall of the junction.

Figure 2(a)-(c) show streamlines in mother and daughter vessels. For low Reynolds numbers (Re = 14), there is no deviation in streamlines while entering the daughter vessel. This is due to the constant velocity distribution in the bifurcation. As the Reynolds number increases, the effect of inertia on blood at the junction point forces blood to accelerate towards the inner wall of the junction as entering the daughter branch; consequently, the density of streamlines increases in this region, and the density of streamlines in the outer wall of the branch decreases. This inhomogeneous distribution of streamlines creates a disturbed region, i.e. region of flow separation, in an arterial branch which is highly susceptible to atherosclerosis. Flow separations at an arterial branch can predispose or contribute to pathogenesis [13]. The primary characteristics of disturbed flows are low average shear stress, constantly changing gradients of shear stress, oscillatory flow (and shear stress) due to flow reversal, and multi-frequency, multidirectional, secondary flows. On the other hand, high shear stress protects against atherosclerosis as long as it remains below the levels that detach the endothelium (*estimated* > 40 pa) [13].

It can be seen from Figure 3(a)-(c) that as the Reynolds number increases, the pressure at the inner region of the junction point increases, and the pressure in the region near the outer wall of the junction point decreases. The reduction of pressure near the outer wall is the result of inertia effects which cause blood molecules to accelerate towards the inner wall. On the other hand, for low Reynolds numbers (Re = 14), the inertia effects can be neglected and the pressure loss near the junction point is negligible. In addition, as can be seen in Figure 3, with the increase of Reynolds number, the pressure in cross-sections of daughter vessels is not constant. Since the theoretical formulas were derived under the assumption of fully developed flow, the increase in Reynolds number reduces the validity of the obtained formulas. Such a phenomenon is best observed at high Reynolds numbers (Re = 1400) in daughters' branches.

Figure 4 depicts the variation of WSS ratio versus Reynolds number for Newtonian fluid. From this figure, it is visible that for low Reynolds numbers, up to 100, WSS ratio is equal to one, meaning that WSS is the same in mother and daughter vessels. This is evidenced through the derived analytical relationships in this article, predicting constant WSS in blood vessel bifurcations with laminar flows. As Reynolds number further increases, the inertia effects overcome viscous effects, leading to an increase in the WSS ratio.

Figure 5 illustrates the variation of flow resistance versus Reynolds number for different ratios of diameter of daughter to mother branches. Also, the volume of branches for different diameter ratios is the same. According to Eq. (10), the optimal diameter is

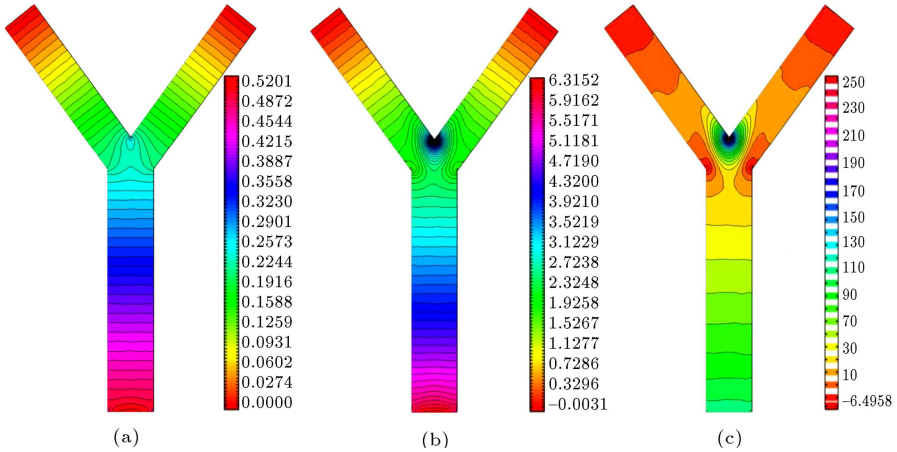

Figure 3. Pressure distribution in aorta geometry with the diameter ratio of 0.8 for (a) Re = 14, (b) Re = 140, and (c) Re = 1400.

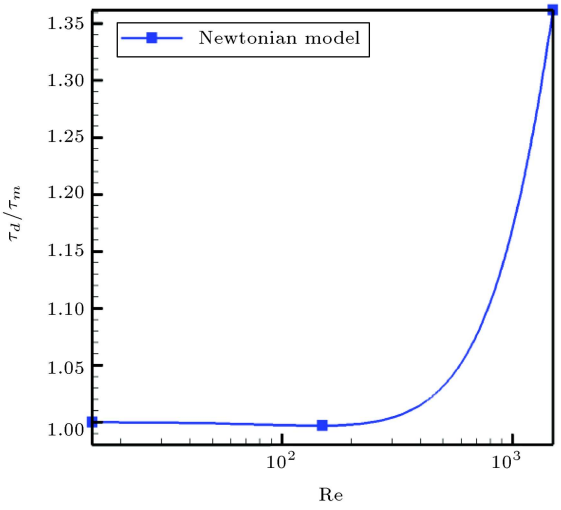

Figure 4. Ratio of WSS of daughter to mother branches with respect to Reynolds number.

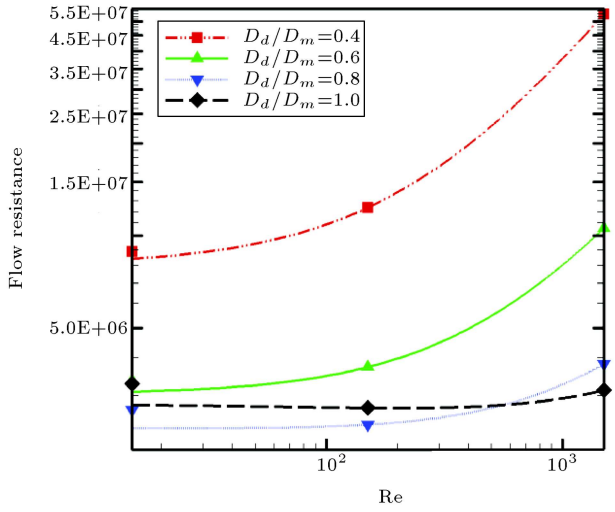

Figure 5. Flow resistance as a function of Reynolds number for different ratios of diameters of mother to daughter vessels.

$D_d/D_m = 2^{-\frac{1}{3}} = 0.8$. It can be seen from Figure 5 that, for a constant ratio of diameters, as the Reynolds number increases, flow resistance increases. It was also observed that for small diameter ratios, the increase in flow resistance is very considerable compared to larger diameter ratios that are close to one.

Figure 6 indicates the variation of flow resistance versus the diameter ratio for different values of the Reynolds number. The non-dimensional flow resistance is the ratio of flow resistance to maximum flow resistance for each Reynolds number given in Figure 5. Also, Figure 6 illustrates the variation of flow resistance with respect to the diameter ratio for constant Reynolds numbers. This figure shows that for small Reynolds numbers, the minimum flow resistance occurs at the diameter ratio of 0.8. In other words, for small Reynolds numbers, the diameter ratio of 0.8 is the optimal geometry configuration leading to a minimum

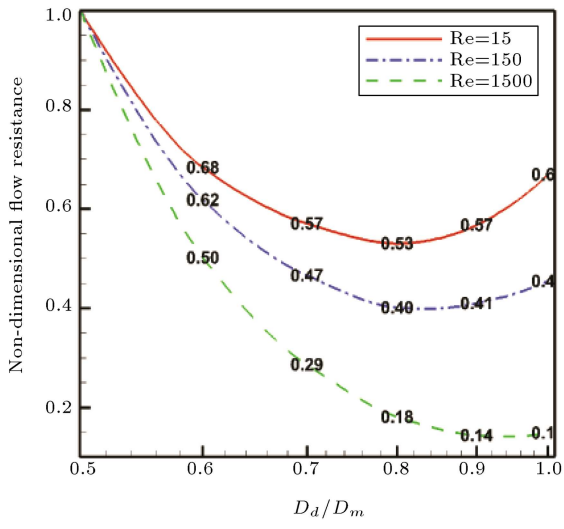

Figure 6. Non-dimensional flow resistance as a function of the ratio of diameters for different Reynolds numbers.

flow resistance. It can be also seen from Figure 6 that for high Reynolds numbers, the simulation calculations predict that minimum flow resistance is likely to happen where the diameter ratio is close to one. Since the inertia effects, such as flow contraction, separation, and secondary flow, are dominant at high Reynolds numbers, equal diameters of mother and daughter branches predict lower flow resistance. However, for low Reynolds numbers, viscous effects are dominant and analytical results are in agreement with numerical ones.

4. Conclusion

In this paper, the optimal distribution of WSS in a bifurcation and its effect on the pattern of diameters of blood vessels were investigated. Using the principle of minimum energy, the optimal WSS was obtained. It was shown that the optimal WSS is a function of metabolic rate, fluid properties, diameter, and flow regime. Different patterns of WSS were obtained for fully developed laminar and turbulent regimes. For laminar flows, WSS was predicted constant through the bifurcation, but for turbulent flows, WSS is a function of diameter, such that the exponent of diameter varies with tube relative roughness. It was shown that, for smooth tubes, the exponent is 6/11, but for fully rough tubes, the exponent is 2/3. Based on the optimal WSS and conservation of mass, the optimal relationship between diameters of mother and daughters vessels was obtained as a function of flow regime. Also, it was theoretically shown that the optimal relationship between diameters of a bifurcation minimizes the flow resistance as well as energy loss. Furthermore, it was shown that the optimal relationship of diameters and a specific relationship between diameter and length of vessels provide the optimal WSS distribution in the bifurcation. Finally, numerical simulation showed that for large Reynolds numbers in the close vicinity of the bifurcation point, WSS in the lateral wall is smaller compared with medial wall. Furthermore, simulation results for symmetrical bifurcation showed that the diameter ratio of 0.8 predicts the minimum flow resistance for low Reynolds numbers, which is in agreement with the analytical results, but diameter ratio equal to one predicts minimum flow resistance for large Reynolds numbers ($\mathrm{Re} = 1400$). Also, it was observed that increasing the Reynolds number is accompanied by increasing the flow resistance. However, this effect becomes less important as diameters' ratio approaches one.

References

1. Murray, C.D. "The physiological principle of minimum work I. The vascular system and the cost of blood volume", *Proceedings of the National Academy of Sciences*, **12**(3), pp. 207-214 (1926).
2. Changizi, M.A. and Cherniak, Ch. "Modeling the large-scale geometry of human coronary arteries", *Canadian Journal of Physiology and Pharmacology*, **78**(8), pp. 603-611 (2000).
3. Sherman, T.F. "On connecting large vessels to small. The meaning of Murray's law", *The Journal of General Physiology*, **78**(4), pp. 431-453 (1981).
4. Beare, R.J., Das, G., Ren, M., et al. "Does the principle of minimum work apply at the carotid bifurcation: a retrospective cohort study", *BMC Medical Imaging*, **11**(1), p. 1 (2011).
5. Razavi, M.S. and Shirani, E. "Development of a general method for designing microvascular networks using distribution of wall shear stress", *Journal of Biomechanics*, **46**(13), pp. 2303-2309 (2013).
6. LaBarbera, M. "Principles of design of fluid transport systems in zoology", *Science*, **249**(4972), pp. 992-1000 (1990).
7. Uylings, H.B.M. "Optimization of diameters and bifurcation angles in lung and vascular tree structures", *Bulletin of Mathematical Biology*, **39**(5), pp. 509-520 (1977).
8. Kassab, Gh.S. "Scaling laws of vascular trees: of form and function", *American Journal of Physiology-Heart and Circulatory Physiology*, **290**(2), pp. H894-H903 (2006).
9. Reneman, R.S., Vink, H. and Hoeks, A.P.G. "Wall shear stress revisited", *Artery Research*, **3**(2), pp. 73-78 (2009).
10. Ingebrigtsen, T., Morgan, M.K., Faulder, K., et al. "Bifurcation geometry and the presence of cerebral artery aneurysms", *Journal of Neurosurgery*, **101**(1), pp. 108-113 (2004).
11. Hahn, J.-Y., Gwon, H.C., Kwon, S.U., et al. "Comparison of vessel geometry in bifurcation between normal and diseased segments: intravascular ultrasound analysis", *Atherosclerosis*, **201**(2), pp. 326-331 (2008).
12. Malek, A.M., Alper, S.L. and Izumo, S. "Hemodynamic shear stress and its role in atherosclerosis", *Jama*, **282**(21), pp. 2035-2042 (1999).
13. Davies, P.F. "Hemodynamic shear stress and the endothelium in cardiovascular pathophysiology", *Nature Clinical Practice Cardiovascular Medicine*, **6**(1), pp. 16-26 (2009).
14. Zamir, M. "Optimality principles in arterial branching", *Journal of Theoretical Biology*, **62**(1), pp. 227-251 (1976).
15. Bejan, A. and Lorente, S. "The constructal law and the evolution of design in nature", *Physics of Life Reviews*, **8**(3), pp. 209-240 (2011).
16. Bejan, A. *Shape and Structure, from Engineering to Nature*, Cambridge University Press (2000).
17. Van der Giessen, A.G., Groen, H.C., Doriot, P.A., et al. "The influence of boundary conditions on wall shear stress distribution in patients specific coronary trees", *Journal of Biomechanics*, **44**(6), pp. 1089-1095 (2011).

18. Moody, L.F. "Friction factors for pipe flow", *Trans. Asme*, **66**(8), 671-684 (1944).

Appendix A

Friction factor and fanning friction factor

Fanning friction factor for fully developed flow through a pipe is defined as follows:

$$C_f = \frac{\tau_w}{\frac{1}{2}\rho V^2}, \tag{A.1}$$

where τ_w is the shear stress at the wall and V is the fluid velocity in the pipe given by $V = \frac{Q}{A}$; Q and A are the volume flow rate through the duct and the cross-sectional area of the duct, respectively. Substituting into Eq. (A.1), we have:

$$C_f = \frac{\tau_w}{\frac{1}{2}\rho Q^2}\left(\frac{\pi}{4}D^2\right)^2. \tag{A.2}$$

The dimensionless friction factor can be written as follows:

$$C_f = \frac{g}{\mathrm{Re}^n} = \frac{g}{\left(\frac{4Q}{\pi \upsilon D}\right)^n}, \tag{A.3}$$

where D is the diameter of the pipe, υ is kinematic viscosity, and the values of constants g and n in Eq. (A.3) are dependent upon the value of the relative roughness of the vessel wall and the value of Reynolds number, Re. The relations between these quantities are depicted in the Moody diagram [18].

The exponent values of D and Q are determined exclusively by n, where $0 \leq n \leq 1$. Value $n = 1$ holds for laminar flow. With the transition from laminar to turbulent flow, the value of n becomes continuously smaller, with $n = 0$ as the limit in the case of completely turbulent flow [7].

Appendix B

Derivation of volumetric flow rate and viscous loss

Based on WSS of conduit and using Eqs. (A.2) and (A.3), the flow rate can be calculated as follows:

$$Q = \lambda\left(\tau_w D^{4-n}\right)^{\frac{1}{2-n}}, \tag{B.1}$$

where $\lambda = (2g\pi^{n-2}\upsilon^n\rho)^{\frac{1}{n-2}}$ is a constant for blood.

A second law of thermodynamic analysis on a conduit's segment of constant cross-section provides the following expression for the power loss due to friction [3,5]:

$$\phi = Q\Delta P. \tag{B.2}$$

For fully developed flow, the momentum balance relates the pressure drop to the shear stress as:

$$\tau_w = \frac{\Delta P}{L}\frac{D}{4}, \tag{B.3}$$

where τ_w is the shear stress at the wall, and ΔP and L refer to pressure drop and length along the conduit, respectively. D is the diameter of conduit.

Using Eqs. (B.1) and (B.3), the power loss due to friction can be expressed as a function of wall shear stress:

$$\phi = \eta L \tau_w^{\frac{n-3}{n-2}} D^{\frac{2}{2-n}}, \tag{B.4}$$

where $\eta = 4 \times (2g\pi^{(n-2)}\upsilon^n\rho)^{\frac{1}{n-2}}$ is a constant.

Appendix C

Derivation of the relationship between mother and daughter vessels for turbulent flow in smooth pipes

One of the purposes of our study is to find a new relationship between mother and daughter vessels with regard to their diameters for turbulent flow in smooth pipes.

For Turbulent flow in smooth pipes, the Blasius correlation, valid for $2 \times 10^3 \leq \mathrm{Re}_D \leq 10^5$, is:

$$f = \frac{0.316}{\mathrm{Re}^{.25}}. \tag{C.1}$$

Fanning friction factor is one-fourth of the Darcy's friction factor ($f = 4C_f$); hence:

$$C_f = \frac{0.079}{\mathrm{Re}^{0.25}}. \tag{C2.}$$

From Eq. (C.2), we can see that the values for g and n are 0.079 and 0.25, respectively. Thus, for turbulent flow in smooth pipes, the extension of Murray's law becomes:

$$D_0^{\left(\frac{27}{11}\right)} = D_1^{\left(\frac{27}{11}\right)} + D_2^{\left(\frac{27}{11}\right)}. \tag{C.3}$$

Appendix D

Derivation of the optimal relationships between diameter and length using minimization of flow resistance

By using Eqs. (B.1) and (B.3), we can derive a relationship between pressure drop and flow rate of a conduit with respect to geometry characteristics as follows:

$$\Delta p = CQ^{2-n}\frac{L}{D^{5-n}}, \tag{D.1}$$

where C is a constant and n is an indicator to determine the flow regime.

With regard to geometry parameters and fluid flow constants, the flow resistance is defined as follows:

$$R_h = C\frac{L}{D^{5-m}}. \tag{D.2}$$

Using the conservation of mass ($Q_0 = Q_1 + Q_2$) and the total pressure drop ($\Delta p = \Delta p_0 + \Delta p_1, \Delta p_1 = \Delta p_2$), the total flow resistance can be expressed as follows:

$$R_h = C\left\{\frac{L_0}{D_0^{5-n}} + \left(\left(\frac{L_1}{D_1^{5-n}}\right)^{\frac{1}{2-n}} + \left(\frac{L_2}{D_2^{5-n}}\right)^{\frac{1}{2-n}}\right)^{n-2}\right\}. \tag{D.3}$$

Using the Lagrange multiplier method to find where R_h is minimized subject to the constraint, that the total volume of conduit is a constant, $\pi(R_0^2L_0 + R_1^2L_1 + R_2^2L_2) = \text{const}$, results in the following equations:

$$\Psi = R_h + \frac{\lambda}{4}(\pi D_0^2 L_0 + \pi D_1^2 L_1 + \pi D_1^2 L_1), \tag{D.4}$$

$$\frac{\partial\psi}{\partial R_0} = 0, \qquad \frac{\partial\psi}{\partial R_1} = 0, \qquad \frac{\partial\psi}{\partial R_2} = 0. \tag{D.5}$$

Elimination of Lagrange multiplier (λ) between Eqs. (D.5) yields the following results:

$$D_0^{\left(\frac{n-7}{n-3}\right)} = D_1^{\left(\frac{n-7}{n-3}\right)} + D_2^{\left(\frac{n-7}{n-3}\right)}, \tag{D.6}$$

$$\frac{L_0}{D_0^{\frac{n+1}{3-n}}} = \frac{L_1}{D_1^{\frac{n+1}{3-n}}}. \tag{D.7}$$

Appendix E

Optimal architecture and minimal flow resistance

In order to find the second necessary condition for optimal WSS, we use conservation of mass ($Q_0 = Q_1 + Q_2$) and total pressure drop ($\Delta p = \Delta p_0 + \Delta p_1, \Delta p_1 = \Delta p_2$) formulas in a bifurcation, in addition to pre-assumption equation (Eq. (9)).

By substituting Eq. (B.3) into Eq. (B.1), volume flow rate in a conduit can be expressed as follows:

$$Q = \omega\left(\frac{LD^{n-5}}{\Delta p}\right)^{\frac{1}{n-2}}, \tag{E.1}$$

where ω is a constant.

From Eq. (E.1), we can obtain the pressure drop as:

$$\Delta P = cQ^{2-m}\left(\frac{L}{D^{5-m}}\right), \tag{E.2}$$

where c is a constant.

By defining $R = c\frac{L}{D^{5-m}}$ and using Eq. (E.1) and conservation of mass, total pressure drop can be obtained as follows:

$$\Delta p = \Delta p_0\left(1 + \frac{R_1R_2}{R_0(R_1+R_2)}\right), \tag{E.3}$$

where R_0, R_1, and R_2 are $\frac{L_0}{D_0^{5-m}}$, $\frac{L_1}{D_1^{5-m}}$, and $\frac{L_2}{D_2^{5-m}}$, respectively.

By substituting pressure drop into Eq. (B.3), solving the equation for WSS of the conduit using Eq. (10), and assuming $\frac{L_0}{D_0^{\frac{n+1}{3-n}}} = \frac{L_1}{D_1^{\frac{n+1}{3-n}}} = \frac{L_2}{D_2^{\frac{n+1}{3-n}}}$, we can find that WSS is optimal.

Consequently, if Eq. (10) exists between mother and daughter vessels, the only assumption that can lead to optimal WSS is $\frac{L_0}{D_0^{\frac{n+1}{3-n}}} = \frac{L_1}{D_1^{\frac{n+1}{3-n}}} = \frac{L_2}{D_2^{\frac{n+1}{3-n}}}$.

Biographies

Matin Golozar graduated with a bachelor's degree in Mechanical Engineering from Isfahan University of Technology and is currently a graduate student at Southern Illinois University, Edwardsville, USA. His Research interests include bioengineering, microfluidics, lab on a chip, BioMEMS, and cardiovascular fluid mechanics.

Mohammad Seyed Razavi received his BSc degree in Mechanical Engineering from Shahrekord University in 2011 and MSc degree in Mechanical Engineering from Isfahan University of Technology in 2013. He is currently a graduate student of Bioengineering at Georgia Institute of Technology, USA. His Research interests lie in the general area of biomechanics and tissue engineering.

Ebrahim Shirani is a PhD from Stanford University in 1981, a Professor Emeritus at Isfahan University of Technology, Isfahan, Iran, and a faculty member at Foolad Institute of Technology, Fooladshar, Isfahan, Iran. His research activities: CFD, turbulence, two phase flows, bio fluid mechanics, micro and nano fluid flows.